International Journal of Pharmaceutics: X 3 (2021) 100104

Contents lists available at ScienceDirect

International Journal of Pharmaceutics: X

journal homepage: www.sciencedirect.com/journal/international-journal-of-pharmaceutics-x

Nanoparticles from Gantrez-based conjugates for the oral delivery of camptothecin

Judit Huarte [a], Socorro Espuelas [a], Cristina Martínez-Oharriz [b], Juan M. Irache [a,*]

[a] Department of Chemistry and Pharmaceutical Technology, NANO-VAC Research Group, University of Navarra, Spain
[b] Department of Chemistry, Faculty of Sciences, University of Navarra, Spain

ARTICLE INFO

Keywords:
Camptothecin
Nanoparticles
Oral delivery
Conjugates
Cyclodextrin
Poly(ethylene glycol)

ABSTRACT

Camptothecin (CPT) exhibits a number of challenges for its oral administration, including a low aqueous solubility, a lactone ring susceptible to hydrolysis, and an affinity to the intestinal P-gp. The aim of this work was to evaluate nanoparticles from Gantrez-based conjugates as carriers for the oral delivery of CPT. For this purpose two different conjugates (G-mPEG and G-HPCD), obtained by the covalent binding of either HP-β-CD or methoxy-PEG (m-PEG) to the polymer backbone of Gantrez™ AN, were synthetized and characterized. Both excipients (m-PEG and HPCD) were selected due to their reported abilities to stabilize the lactone ring of CPT and disturb the effect of intestinal P-gp. The resulting nanoparticles (G-mPEG-NP and G-HPCD-NP) presented a similar size (about 200 nm) and zeta potential (close to −35 mV); although, G-mPEG-NP presented a higher CPT payload than G-HPCD-NP. On the contrary, in rats, nanoparticles based on Gantrez conjugates appeared to be capable of crossing the protective mucus layer and reach the intestinal epithelium, whereas conventional Gantrez nanoparticles displayed a mucoadhesive profile. Finally, the pharmacokinetic study revealed that both formulations were able to enhance the relative oral bioavailability of CPT; although this value was found to be 2.6-times higher for G-mPEG-NP than for G-HPCD-NP.

1. Introduction

Camptothecin (CPT) is a quinolone based alkaloid that was isolated from the bark of *Camptheca acuminate* tree (Dev et al., 2016). The antitumor activity of CPT is mainly due to its interaction with and blocking effect of Topoisomerase 1 (Top 1), a ubiquitous and essential enzyme required for DNA transcription and replication (Li et al., 2017). In the cell, CPT would be integrated into the complex formed by Top 1 and DNA (Top1-DNA complex) through hydrogen bonding. The formation of this ternary complex would prevent the relegation of the nicked DNA, as well as the dissociation of the Top 1-DNA complex (Champoux, 2001; Pommier, 2006). Furthermore, during the replication phase, this ternary complex would act as an obstacle for the replication fork, inducing DNA double-strand breaks and cell death. Both Top1 and DNA are required for CPT binding, and CPT does not have significant binding to either in the absence of the other (Liu et al., 2000; Li et al., 2006). Apart from this main mechanism, CPT would also affect the activity of cellular proteins and RNA and DNA synthesis (Li et al., 2017). In preclinical studies camptothecin, has been shown to be effective against human xenografts of colon, lung, breast, ovarian, and melanoma cancers (Van Hattum et al., 2002; De Cesare et al., 2004; Li et al., 2017).

Nevertheless and in spite of the promising results at the preclinical level, clinical trials demonstrated an unexpected toxicity and low antineoplastic activity (Venditto and Simanek, 2010; Botella and Rivero-Buceta, 2017). In fact, camptothecin exhibits a number of challenges for its formulation and administration. Firstly, camptothecin shows a very low aqueous solubility (approximately 4 μg/mL) (Saetern et al., 2004). Secondly, the chemical structure of camptothecin includes an unstable lactone ring that is highly susceptible to spontaneous and reversible hydrolysis, under physiological pH conditions, yielding a hydrophilic and inactive (but more toxic) carboxylate form (Lorence and Nessler, 2004; Adane et al., 2012). These two forms of camptothecin (lactone and carboxylate) co-exist at 50% at a pH of 6.65. At pH below 6.65, the equilibrium moves towards the lactone and active form of CPT whereas, under neutral and basic pH conditions, the carboxylate derivative predominates (Venditto and Simanek, 2010). In addition, camptothecin is also a P-glycoprotein substrate (Takemoto et al., 2006; Negi et al., 2013), which hampers its oral administration.

* Corresponding author at: Dep. Chemistry and Pharmaceutical Technology, NANO-VAC Research Group, University of Navarra, C/ Irunlarrea, 1, 31008 Pamplona, Spain.
E-mail address: jmirache@unav.es (J.M. Irache).

https://doi.org/10.1016/j.ijpx.2021.100104
Received 23 September 2021; Received in revised form 5 November 2021; Accepted 6 November 2021
Available online 9 November 2021

In order to solve some of these drawbacks, structural modifications of the camptothecin chemical structure have been implemented. These works led to the synthesis of a number of camptothecin analogues and, at least two of them (i.e., topotecan and irinotecan), have been approved by the Regulatory Agencies and are currently employed for the treatment of different types of cancer (Oberlies and Kroll, 2004). In a different approach, conjugates between camptothecin and either poly (ethylene glycol) (PEG) or cyclodextrins have also been proposed. One example would be Pegamotecan, a water-soluble macromolecule consisting of two camptothecin molecules conjugated, by an alaninate ester linkage, to a 40 kDa PEG (Li and Wallace, 2008). This linkage stabilizes the CPT molecule into its active lactone conformation (Zhang and Ma, 2013). Another interesting camptothecin conjugate is CRLX-101. This derivative is composed by PEG, di-substituted β-cyclodextrin moieties and CPT linked through a glycine ester linkage, and has also shown promising results in clinical trials (Sanoff et al., 2019).

Another interesting strategy to solve the inconveniences of camptothecin and facilitate its oral administration would be its encapsulation in nanocarriers, including lipid-based nanoparticles (Yang et al., 1999; Du et al., 2018), dendrimers (Sadekar et al., 2013), and polymer nanoparticles (Huarte et al., 2016; Ünal et al., 2020). In this context, an alternative to increase the oral absorption of this drug may be its encapsulation in nanoparticles capable of diffusing through the mucus layer and, then, of reaching the mucosal epithelium surface in order to increase their residence time in close contact with the absorptive membrane. Such oral formulation could offer prolonged and sustained levels of the drug in plasma and, indeed, an improved pharmacokinetic profile that would facilitate the therapeutic use of this drug.

For this purpose, we propose in this work two different types of nanoparticles from conjugates based on the copolymer of methyl vinyl ether and maleic anhydride (Gantrez™ AN). This copolymer is highly soluble in acetone but insoluble in ethanol and water. However, in contact with water the polymer is hydrated leading to hydrolysis and subsequent dissolution. Moreover, the presence of highly reactive anhydride residues, facilitates the polymer customization with a large variety of nucleophiles (i.e., hydroxyl and primary amine groups) and would endow nanoparticles with modified properties including their capability to load lipophilic drugs and/or improved biodistribution abilities. In this context, hydroxypropyl-β-cyclodextrin and poly (ethylene glycol)s may be of interest to combine with Gantrez™ AN in order to obtain polymeric conjugates that, transformed into nanoparticles, would be capable of yielding adequate formulations for the oral delivery of camptothecin. In fact, both excipients can stabilize the CPT's lactone ring (Swaminathan et al., 2010; Ci et al., 2013) and have been described as inhibitors of the intestinal P-gp efflux pump (Werle, 2008; Zhang et al., 2011; Nguyen et al., 2021).

Therefore, the aim of this work was, in a first step, to synthesise and characterize new cyclodextrin- or poly(ethylene glycol)-Gantrez™ AN conjugates. Then, in a second step, these conjugates were used to prepare CPT-loaded nanoparticles. Finally, a pharmacokinetic study after the oral administration of these nanoparticles to Wistar rats was carried out.

2. Materials and methods

2.1. Materials

Poly(methyl vinyl ether-*co*-maleic anhydride) or poly(anhydride) (Gantrez™ AN 119; MW 200,000) was purchased from Ashland Inc. (KY, USA). Camptothecin (CPT) (99.0%) was supplied by 21CECpharm (London, UK). 2-hydroxypropyl-β-cyclodextrin (HP-β-CD), methoxy poly(ethylene glycol) 2000 (mPEG), Lumogen® red, DAPI (4′,6-diamidino-2-phenylindole), solid iodine (≥99.8%), pepsin and pancreatin were obtained from Sigma-Aldrich (Germany). Tissue-Tek® OCT compound was purchased from Sakura, The Netherlands. Acetone, ethanol, acetonitrile, formaldehyde, tetrahydrofuran (THF) and trifluoroacetic acid (TFA) were obtained from Merk (Darmstadt, Germany). All other reagents and chemicals used were of analytical grade and supplied from Sigma Aldrich (MO, USA) and Merck (Darmstadt, Germany).

2.2. Preparation of poly(anhydride) based-conjugates

Two different types of polymer conjugates, based on the combination of either mPEG or HP-β-CD with Gantrez™ AN 119 (Gantrez), were prepared.

2.2.1. Preparation of poly(anhydride)-metoxiPEG2000 conjugate (G-mPEG)

For the preparation of G-mPEG, 500 mg Gantrez were firstly dissolved in 300 mL acetone and heated at 50 °C. In parallel, a variable amount of mPEG (mPEG-to-Gantrez ratios between 0.05 and 0.2 by weight) was dissolved in 100 mL acetone and, then, added dropwise to the Gantrez solution. The mixture was maintained under magnetic agitation for 4 h and, then, the solvent was eliminated under reduced pressure (Büchi R210, Switzerland). The residue was dispersed in 20 mL dicloromethane and the mixture sonicated for 1 min. The residue was collected and the supernatants analysed by TLC, using a mixture of dicloromethane and methanol (9:1 by vol.) as mobile phase and solid iodine as reagent to identify the presence of free PEG. This purification step was repeated two times.

2.2.2. Preparation of poly(anhydride)-HPCD conjugates (G-HPCD)

In this case, 500 mg Gantrez were dissolved in 300 mL acetone, whereas 100 mg of HP-β-CD was dispersed in 100 mL of the same solvent. Then, the oligosaccharide mixture was added dropwise to the polymer solution heated at 50 °C. The mixture was maintained under magnetic stirring at the same temperature for 4 h. The mixture was filtered in order to eliminate the remaining free cyclodextrin and the filtrate was evaporated under reduced pressure. Finally, the solid was collected and purified as described above.

2.3. Characterization of the conjugates

Gantrez-based conjugates were characterized to confirm the binding of either mPEG or HP-β-CD to the polymer backbone, as well as to calculate the molecular weight (MW) and the degree of substitution.

2.3.1. Infrared spectroscopy (IR)

IR spectroscopy was performed in a Nicolet Avatar 360FT-IR apparatus (Thermo, WI, USA) to confirm the presence of carbonyl groups and, then, to evidence the opening of the anhydride group in the Gantrez backbone (Lucio et al., 2018).

2.3.2. Nuclear magnetic resonance spectroscopy (^{1}H NMR)

^{1}H-RMN studies were carried out in an Avance 400 apparatus (Bruker, WI, USA) of 400 MHz, using a pulse program of zg30 and a waiting time between pulses (D_0) of 1 s. The number of accumulations was 64. The samples (2 mg) were analysed after dissolution in 0.5 mL deuterated acetone as solvent. The integration of the signal corresponding to the methylated proton in the Gantrez (δHa at 4.25 ppm in Fig. S1, Supplementary material) was used as reference. For mPEG and HP-β-CD, the reference signals were bands produced by protons identified with δHa′ at 3.6 ppm (Supplementary material, Fig. S2) and δHa″ at 3 ppm, respectively (Supplementary material, Fig. S3). The amount of either mPEG or HP-β-CD bound to the polymer backbone in the synthetized conjugates was then estimated using the following δHa-to-δHa′ and δHa-to-δHa″ ratios.

2.3.3. Titration

Gantrez and the synthetized conjugates were dispersed in water in order to induce a complete hydrolysis of anhydride groups (about 24 h). Then, aqueous solutions of the hydrolysed polymers were titrated with a

NaOH 0.2 N solution in the presence of phenolphthalein.

2.3.4. Dynamic light scattering

DLS analysis was performed at a scattering angle of 90° using a DynaPro-MS/X photon correlation spectrometer equipped with a 248-channel multi-tau correlator and a Peltier effect temperature unit (Proteins solutions Inc., USA). The wavelength of the laser was 852.2 nm at 100% intensity. Measurements were carried out at 25 °C after dissolving the conjugates in tetrahydrofurane.

2.3.5. Elemental analysis

Conjugates were analysed in a CHN-900 Leco apparatus (Leco Corporations, USA) in order to determine their composition in carbon, hydrogen, oxygen and nitrogen.

2.4. Preparation of camptothecin-loaded nanoparticles

Camptothecin-loaded nanoparticles from the synthetized conjugates were prepared by a desolvation procedure described previously (Huarte et al., 2016) with some modifications. For this purpose, 100 mg of either G-mPEG or G-HPCD were dissolved by magnetic stirring in 4 mL acetone. On the other hand, 3 mg CPT were dispersed in 1 mL acetone and sonicated for 30 s before introduction in the organic solution of the conjugate. Nanoparticles were obtained by the addition of a hydro-alcoholic solution (50% ethanol, containing calcium chloride 0.8% *w/v*). The organic solvents were eliminated under reduced pressure (Büchi R210, Switzerland) and the suspension of nanoparticles were filtered through a 0.45 µm membrane before centrifugation at 27,000 x*g*, for 20 min in a 3 K30 centrifuge (Sigma Centrifuges, UK). The resulting pellets were resuspended in water and freeze-dried (Genesis 12EL, Virtis, USA) using sucrose (5% w/v) as cryoprotectant.

The developed formulations were named as follows: G-mPEG-NP, camptothecin-loaded nanoparticles obtained from G-mPEG; G-HPCD-NP, camptothecin-loaded nanoparticles obtained from G-HPCD. Empty nanoparticles were prepared in the same way as described above but in the absence of camptothecin (empty G-mPEG-NP and empty G-HPCD-NP).

On the other hand, for the distribution studies, nanoparticles containing Lumogen® red were prepared by adding 0.5 mg of the fluorescent dye in the acetone (5 mL) containing the conjugate. Then, the nanoparticles were prepared as described above. Finally, control Gantrez nanoparticles, fluorescently loaded with Lumogen® red, were also prepared by inducing the desolvation of the polymer with a hydro-alcoholic solution (50% ethanol) in the absence of calcium chloride.

2.5. Characterization of CPT-loaded nanoparticles

2.5.1. Physicochemical characterization

The diameter and the zeta potential of nanoparticles were determined in a ZetaPlus analyzer system (Brookhaven Instruments Corp., New York, USA). The diameter of the nanoparticles was determined after dispersion in water (1:10), whereas the zeta potential was determined after dispersion of nanoparticles in 0.1 mM KCl solution. The morphology of the nanoparticles was examined by scanning electron microscopy (SEM) in a Zeiss DSM940 digital scanning electron microscope (Oberkochen, Germany) coupled with a digital image system (Point Electronic GmBh, Germany). The yield of the process was calculated by gravimetry as described previously (Arbós et al., 2002).

2.5.2. Camptothecin analysis

The amount of CPT-loaded into nanoparticles was quantified by HPLC-FLD (Huarte et al., 2016). The cromatographic system was mounted with a reversed-phase 150 mm × 3 mm C18 Phenomenex Gemini column (particle size 5 µm) and precolumn (Phenomenex SecurityGuard C18). The mobile phase, at a flow rate of 1 mL/min, was a mixture of acetonitrile and trifluoroacetic acid 0.01% in water (1:1 by vol.). The detection was performed by fluorescence in a detector set at excitation and emission wavelengths of 380 and 418 nm, respectively. The injection volume was 20 µL. Calibration curves were designed over the range of 0.48 and 8000 ng/mL ($R^2 > 0.999$). The limit of quantification was calculated to be 1.3 ng/mL with a relative standard deviation of 4.1%.

For analysis, the amount of free CPT was measured in the supernatants obtained after ultracentrifugation of an aqueous suspension of lyophilized nanoparticles in water. In parallel, the total amount of CPT in the lyophilized samples was quantified by HPLC after dispersion and breaking down of lyophilized nanoparticles in acetonitrile. Each sample was assayed in triplicate and results were expressed as the amount of CPT (in µg) per mg nanoparticles.

2.6. In vitro release studies

In vitro release experiments were conducted under sink conditions at 37 °C using simulated gastric (SGF; pH 1.2; containing pepsin) and intestinal (SIF; pH 6.8; containing pancreatin) fluids. Studies were performed under agitation in a Vortemp 56™ Shaking Incubator (Labnet International Inc., NJ, USA). For each time point, nanoparticles (containing 0.8 µg CPT) were dispersed in 1 mL of the corresponding simulated fluid and, at different time-points, transferred to Vivaspin tubes (300,000 MWCO, Sartorius group, Germany) before centrifugation at 3000 ×*g* for 5 min. The supernatants were analysed by HPLC (see Section 2.5.2) and the release profiles expressed in terms of CPT cumulative release (in percentage).

2.7. In vivo distribution study of con-mPEG2-NP and con-HPCD-NP in the gut mucosa

In order to visualize and evaluate the distribution and the capability of the nanoparticles to interact with the gut mucosa, fluorescence microscopy studies were carried out (Inchaurraga et al., 2019). Animal experiments were performed in male Wistar rats following a protocol approved by the Ethical and Biosafety Committee of the University of Navarra in agreement with the European legislation on animal experiments (protocol number 059–13). Each animal received orally a single dose of fluorescently labelled nanoparticles (10 mg in 1 mL water). Two hours later, the animals were sacrificed and the ileum portions of 1 cm were collected, stored in the tissue proceeding medium Tissue -Tek® OCT and frozen at −80 °C. Finally, samples of intestinal sections with a thickness of 5 µm were treated with formaldehyde and incubated with DAPI (4′,6-diamidino-2-phenylindole) for 15 min before the visualization of the fluorescence in a microscope (Axioimager M1, Zeiss) with a coupled camera (Axiocam ICc3, Zeiss) and fluorescent source (HBO 100, Zeiss).

2.8. In vivo pharmacokinetic studies

Pharmacokinetic studies were performed in Wistar rats obtained from Harlan (Barcelona, Spain) and conducted in accordance with the ethical guidelines and policies for investigations in laboratory animals approved by the Ethical Committee for Animal Experimentation of the University of Navarra (protocol number 058–12). Before the oral administration of the formulations, animals were fasted overnight, allowing free access to water. Two experimental groups of six animals each were prepared: (a) G-mPEG-NP, and (b) G-HPCD-NP. Nanoparticles were dispersed in 1 mL water and administered as a single dose of 1 mg CPT/kg bw. Control animals ($n = 6$) received orally the same volume of a CPT aqueous suspension (1 mg/kg). The camptothecin suspension was prepared extemporary by dispersing the drug (3.6 mg) in 10 mL of a solution of Tween 80 and NaCl 0.9% (9:1) in water (Fox et al., 2009).

Blood samples were collected at different times and the blood volume was recovered ip with an equal volume of saline solution pre-

heated at body temperature. Samples were immediately centrifuged at 2500 xg for 10 min and the plasma was frozen at -20 °C until analysis.

2.8.1. Determination of CPT plasma concentration by HPLC-FLD

The amount of CPT was determined in plasma by HPLC and fluorescence detection with the technique described above (see Section 2.5.2). In this case, the injection volume was 100 µL. Calibration curves (in the range of 0.48 and 8000 ng/mL; $R^2 > 0.999$) were prepared by adding a solution of camptothecin in a mixture of dimethylsulfoxide, acetonitrile and trifluoroacetic acid (1:8.9:0.1 by vol.) to drug free plasma. The limit of quantification was calculated to be 2.6 ng/mL with a relative standard deviation of 4.6%.

For analysis, an aliquot of plasma (100 µL) was mixed with 400 µL acetonitrile and vortexed for 2 min. After centrifugation (5000 xg, 5 min), the supernatant was evaporated until dry and the residue dissolved in 120 µL of reconstitution solution (dimethylsulfoxide, acetonitrile and trifluoroacetic acid; 1:8.9:0.1 *v*/v/v) before analysis.

2.8.2. Pharmacokinetic data analysis

The pharmacokinetic analysis was performed using a non-compartmental model with the WinNonlin 5.2 software (Pharsight Corporation, USA). The following parameters were estimated: maximal plasmatic concentration (C_{max}), time in which the maximum concentration is reached (T_{max}), area under the concentration-time curve from time 0 to t h (AUC), clearance (Cl), volume of distribution (V) and half-life in the terminal phase ($t_{1/2}$). Furthermore, the relative oral bioavailability, Fr, of CPT was expressed as the ratio between the area under the concentration-time curve from time 0 to t (AUC) of the formulations assayed and the one of the oral suspension of CPT administered.

2.9. Statistical analysis

Statistical analysis was performed using GraphPad Prism 5.0 statistical software (GraphPad Software, USA). For the in vivo study, the non-parametric Kruskall-Wallis followed by Mann-Whitney *U* test was employed to investigate statistical differences ($p < 0.05$ was considered as statistically significant difference).

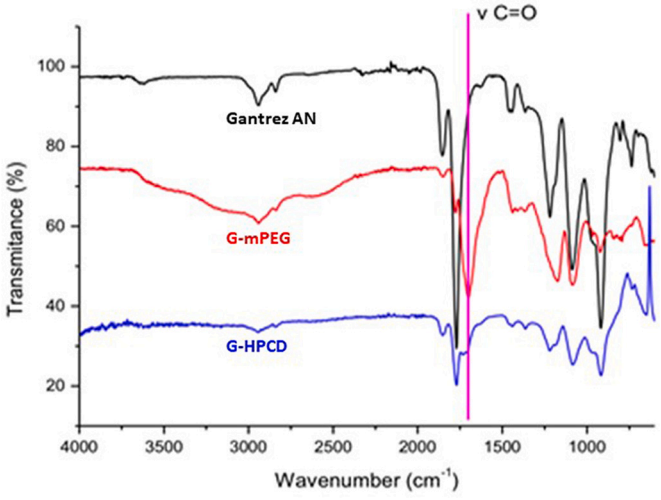

Fig. 1. IR spectra of Gantrez and its conjugates with either mPEG (G-mPEG) or HP-β-CD (G-HPCD). Synthesis experimental conditions: excipient-to-Gantrez ratio of 0.2; incubation time 4 h; 50 °C.

3. Results

3.1. Characterization of the conjugates

Fig. 1 shows the IR spectra of the conjugates between Gantrez and either mPEG or HP-β-CD. In the spectrum of both compounds (G-mPEG and G-HPCD) a new band (at ~1705 cm^{-1}) appeared. This band would be associated with the stretching of the carbonyl group ($\nu_{C=O}$), suggesting a nucleophilic substitution reaction between hydroxyl groups of either mPEG or HP-β-CD and the anhydride residues of Gantrez; yielding new ester bonds (Mazo et al., 2011).

Supplementary material (Figs. S4 and S5) contains the spectra obtained from the analysis of conjugates by ^{1}H-RMN, compared to those of Gantrez, mPEG and HP-β-CD. From these spectra, the amount of mPEG or HP-β-CD bound to the poly(anhydride) backbone, as well as the substitution degree (DS), were calculated (Table 1). For mPEG based-conjugates, higher mPEG-to-Gantrez ratios in the synthesis lead to higher percentages of mPEG bound to the polymer backbone. Thus, at a mPEG-to-Gantrez ratio of 0.05, the DS was calculated to be of 5.7%, whereas at a ratio of 0.2, the DS reached a value of 9.5%. For HP-β-CD-based conjugates, since the reaction was carried out by dispersing the cyclodextrin in the organic solution of Gantrez, increasing cyclodextrin-to-Gantrez ratios did not lead to higher substitution degrees (data not shown). Under these experimental conditions, the DS was calculated to be of about 8.8%.

Table 2 shows the percentage of free carboxylic groups of conjugates and Gantrez calculated by titration after complete hydrolysis and dissolution in water. Interestingly, for both conjugates, the amount of –COOH groups was around 50% of the carboxylic groups estimated for Gantrez. On the other hand, the hydrodynamic radius of Gantrez when dissolved in tetrahydrofurane was close to 19. This value was slightly lower for G-mPEG (around 13), whereas for G-HPCD the hydrodynamic radius was 10 times higher than that of the original polymer (Table 2). Regarding the elemental analysis (Table 2), the binding of either mPEG or HP-β-CD to the polymer backbone, decreased the percentage of carbon and increased the oxygen content. This decrease in the C-to-O ratio (C/O ratio) was higher for G-mPEG than for G-HPCD.

3.2. Characterization of camptothecin-loaded nanoparticles

The physicochemical characteristics of the resulting conjugate-based nanoparticles are summarized in Table 3. Empty nanoparticles, independently of the conjugate employed, displayed similar mean sizes (about 250 nm) and negative zeta potential (between −33 and −38 mV). For both types of nanocarriers, the yield of the process, expressed as the amount of polymer (either G-mPEG or G-HPCD) transformed into nanoparticles, was calculated to be close to 80%.

For camptothecin-loaded nanoparticles, the mean size and the yield of the process was slightly lower than for the empty ones (Table 3). Interestingly, the encapsulation of camptothecin did not modify the zeta potential of the resulting nanoparticles. On the other hand, nanoparticles form G-mPEG displayed a higher capability to load camptothecin than G-HPCD-NP (11 vs 8.6 µg/mg; $p < 0.05$).

The morphological analysis by scanning electron microscopy (Fig. 2)

Table 1
Estimated molecular weight (MW) and degree of substitution (DS) for the different conjugates synthesised calculated by ^{1}H NMR. The MW of Gantrez™ AN (as defined by the manufacturer) was 216 kDa.

	Excipient-to-Gantrez ratio	MW (g/mol)	DS (%)
Gantrez	–	216,000	–
G-mPEG	0.05	229,099	5.7
G-mPEG	0.1	230,165	6.2
G-mPEG	0.2	238,694	9.5
G-HPCD	0.2	236,770	8.8

Table 2
Physico-chemical characterization of Gantrez and its conjugates with either mPEG or HP-β-CD. Determination of carboxylic acids by titration and hydrodynamic radius (Rh) by DLS. Synthesis experimental conditions: excipient-to-poly(anhydride) ratio of 0.2; incubation time 4 h, 50 °C.

	%COOH	Rh	%C	%H	%O	C/O ratio
Gantrez	100	18.96	53.49	5.18	41.33	1.29
G-mPEG	50.27	12.89	48.33	6.01	45.66	1.06
G-HPCD	48.36	134.97	51.46	5.33	43.21	1.19

Table 3
Physico-chemical characterization of nanoparticles based on the synthetized conjugates. Empty nanoparticles were manufactured without CPT. G-mPEG-NP, camptothecin-loaded nanoparticles obtained with G-mPEG; G-HPCD-NP, camptothecin loaded nanoparticles prepared with G-HPCD. Data expressed as mean ± SD, $n > 3$.

	Mean size (nm)	PDI	Zeta potential (mV)	Yield (%)	CPT loading (μg/mg)
Empty G-mPEG-NP	250 ± 6	0.20 ± 0.04	-33 ± 4	81 ± 5	–
Empty G-HPCD-NP	245 ± 7	0.19 ± 0.05	−38 ± 6	83 ± 4	–
G-mPEG-NP	195 ± 2	0.23 ± 0.03	−36 ± 3	69 ± 4	10.9 ± 0.2
G-HPCD-NP	230 ± 10	0.24 ± 0.04	−33 ± 2	73 ± 7	8.6 ± 1.2

showed that both types of nanoparticles (G-mPEG-NP and G-HPCD-NP) consisted of homogeneous populations of spherical particles of a size similar to that obtained by photon correlation spectroscopy. Moreover, in both cases, the surface of nanoparticles appeared to be smooth.

3.3. In vitro release study

Fig. 3 represents the release profiles of camptothecin from G-mPEG-NP and G-HPCD-NP in simulated gastric and intestinal fluids, as cumulative percentage of drug released as a function of time. Both formulations, showed a similar release profile. In SGF, during the first 2 h of the experiment, the amount of camptothecin released from nanoparticles was very low (about 10% for G-mPEG-NP and 20% for G-HPCD-NP). On the contrary, in SIF, CPT was rapidly released from nanoparticles. In fact, after one hour of incubation in SIF, more than 80% of the initial drug loaded was released from the two nanoparticle formulations.

3.4. In vivo distribution study of G-mPEG-NP and G-HPCD-NP in the gut mucosa

For the in vivo distribution study, nanoparticles were fluorescently labelled by encapsulation of lumogen red. The resulting nanoparticles displayed similar physico-chemical properties to those determined for empty nanoparticles (data not shown). Fig. 4 A and B show the distribution of Gantrez nanoparticles fluorescently labelled with lumogen red (215 nm and −36 mV) in the ileum of rats, two hours after their oral administration as single dose. These control nanoparticles displayed a distribution that appeared to be restricted to the mucus layer covering the intestinal epithelium. On the other hand, nanoparticles made from G-mPEG appeared to be able to cross the mucus layer and interact in a more intimate way with the surface of the enterocytes (Fig. 4C and D). Similarly, nanoparticles from G-HPCD also displayed a higher capability than Gantrez nanoparticles to reach the absorptive membrane of the intestinal epithelium; although, in this case a fraction of the formulation was also trapped in the mucus layer (Fig. 4E and F).

3.5. Pharmacokinetic studies

Fig. 5 shows the plasma concentration profiles of CPT after the oral administration to rats of a single dose (1 mg/kg) as either a suspension

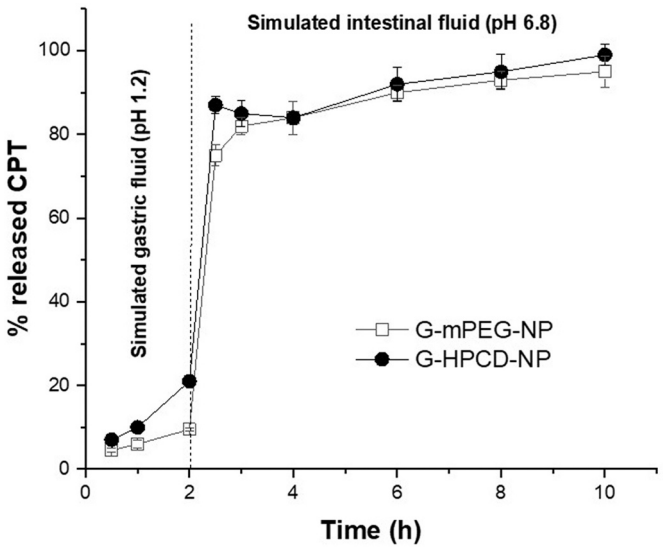

Fig. 3. Camptothecin release profile from G-mPEG-NP and G-HPCD-NP after incubation in simulated gastric fluid (0−2*h*) and simulated intestinal fluid (2–14 h) under sink conditions. Data expressed as mean ± SD, $n = 3$.

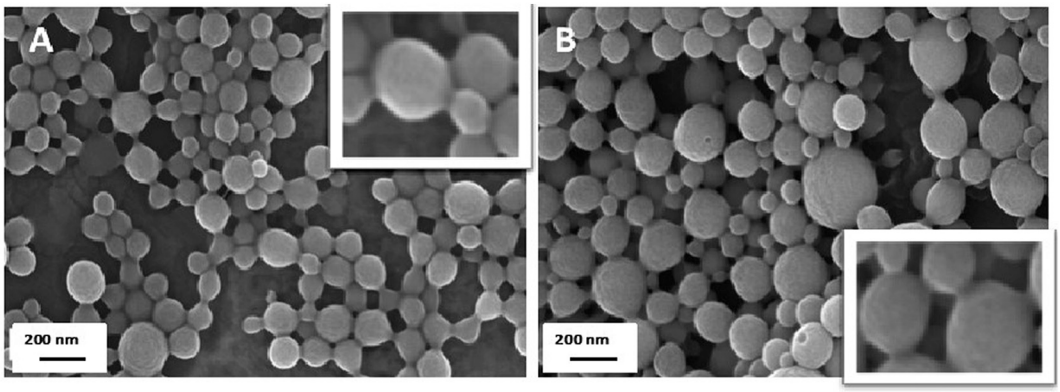

Fig. 2. Scanning electron microscopy (SEM) of freeze-dried nanoparticles. A: G-mPEG-NP. B: G-HPCD-NP.

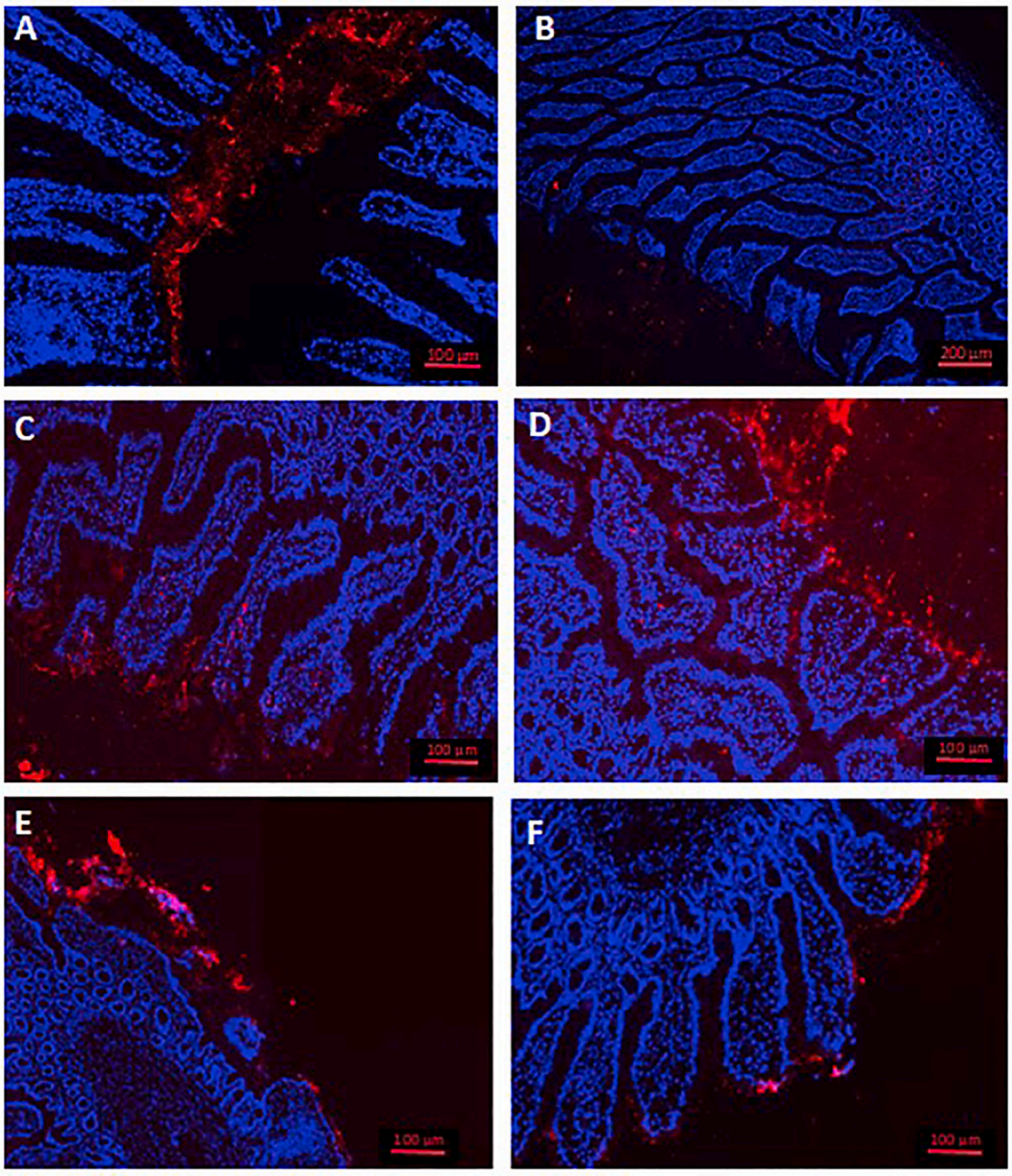

Fig. 4. Visualization of nanoparticles based on Gantrez (A and B), G-mPEG (C and D) and G-HPCD (E and F), fluorescently labelled with lumogen red, in the proximal ileum of rats. Cell nuclei of enterocytes dyed with DAPI (in blue). (For interpretation of the references to colour in this figure legend, the reader is referred to the web version of this article.)

or loaded in nanoparticles. Table 4 summarises the main pharmacokinetic parameters estimated with a non-compartmental analysis of the experimental data. For the control formulation (suspension of camptothecin), the drug plasma levels increased rapidly reaching the C_{max} 30 min after administration. Eight hours post-administration the CPT plasma levels were close to 15 ng/mL and, two-hours later, not detectable levels were found.

For camptothecin-loaded nanoparticles, the initial profile of the plasma curve was quite similar to that observed for the camptothecin suspension; however, these levels were maintained in a sustained way for at least 48 h post-administration. Overall, the plasma levels of camptothecin from G-mPEG-NP were higher than those observed from G-HPCD-NP. Interestingly, G-mPEG-NP displayed a more moderate decrease of drug levels in plasma, resulting in an AUC 2.6-times higher than the AUC obtained after the administration of G-HPCD-NP (Table 4). For nanoparticles based on Gantrez-conjugates, in both cases, the camptothecin AUC was significantly higher than for the aqueous suspension of the drug ($p < 0.05$). In a similar way, for G-mPEG-NP and G-HPCD-NP, the half-life of the terminal phase of the curve ($t_{1/2}$) was also significantly higher than for the control formulation. In accordance with these results, the clearance of the drug when administered in G-mPEG-NP was about 11-times lower than the value obtained when administered as a suspension ($p < 0.01$). This decreased clearance was also observed when camptothecin was encapsulated in G-HPCD-NP; although, in this case, the difference was also of 3.5 times lower ($p < 0.05$). Finally, the relative oral bioavailability of camptothecin when loaded in G-mPEG-NP and G-HPCD-NP was almost 8- to 3-fold higher than when prepared as an aqueous suspension, respectively.

4. Discussion

Oral chemotherapy's interest has grown through the last years due to the benefits it offers to the patient and its economical sustainability. However, in this field, the oral route holds great problems, being the

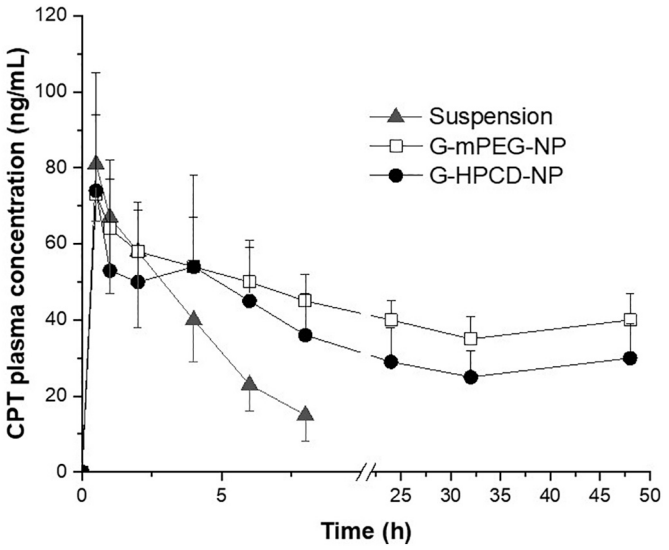

Fig. 5. Concentration-time profile of camptothecin in male Wistar rats after a single oral dose (1 mg/kg) of a drug aqueous suspension, or the equivalent CPT formulated in con-mPEG2-NP and con-HPCD-NP. Data expressed as mean (±SD), ($n = 6$).

bioavailability of most of anticancer drugs one of the most challenging. Camptothecin, a molecule with powerful anticancer activity, shows poor water solubility and it is substrate of the P-glycoprotein (Sadekar et al., 2013). In addition, CPT shows a low metabolic stability directly related with a rapid hydrolysis of its lactone ring under physiological conditions (Venditto and Simanek, 2010; Malhotra et al., 2021). These drawbacks have hindered up to date every attempt of its administration, preventing it from being approved for use in clinic.

In order to overcome these issues, our strategy was to prepare and evaluate nanoparticles to carrying the loaded drug to the surface of the absorptive membrane of enterocytes. For this purpose, the use of nanoparticles from hydrophilic conjugates (based on the binding of either HP-β-CD or mPEG to the polymer backbone of Gantrez) may be of interest. This selection was based on the capability of both excipients (HP-β-CD or mPEG) to stabilize the camptothecin lactone ring (Swaminathan et al., 2010; Ci et al., 2013) and disturb the activity of the intestinal P-gp efflux pump (Werle, 2008). In the past, we have demonstrated that pegylation of Gantrez nanoparticles may be an adequate approach to confer mucus-permeating properties and improve the oral bioavailability of lipophilic drugs (Inchaurraga et al., 2015; Ruiz-Gatón et al., 2018). However, in these works, high PEG-to-Gantrez nanoparticles ratios were necessary to obtain adequate PEG coating layers. As a result, the purification step of the nanoparticles involved important challenges. On the other hand, the encapsulation of cyclodextrin-drug complexes (instead of the free drug) may increase the payload of the resulting nanoparticles as well as the bioavailability of the loaded drug (Calvo et al., 2011; Huarte et al., 2016). However, due to the use of organic solvents for the preparation of these nanoparticles, the physico-chemical stability of the complexes may be compromised; minimizing the expected advantages from the presence of the cyclodextrin. One alternative to solve these inconveniences may be the preparation of nanoparticles directly from the polymer conjugate, previously synthetized and characterized, rather than the implementation of more complex preparative processes organized around several steps.

In the synthetized conjugates, the covalent binding of either mPEG or HP-β-CD to the Gantrez was evidenced by IR (Fig. 1) and corroborated by ^{1}HNMR (Supplementary material), elemental analysis and titration experiments (Tables 1 and 2). For G-mPEG conjugates, the highest degree of substitution of Gantrez was found with a mPEG-to-poly (anhydride) ratio of 0.2. Under these experimental conditions, the degree of substitution was calculated to be about 95 μg mPEG per mg conjugate. For G-HPCD conjugates, the degree of substitution was lower than for G-mPEG (about 8.8%); probably due to the insolubility of the cyclodextrin under the conditions in which the reaction was carried out.

Nanoparticles from both G-mPEG and G-HPCD were prepared by a simple desolvation method with an ethanol-water mixture (1:1 by vol) in the presence of calcium chloride. The presence of calcium enabled us to increase the yield of the preparative process (data not shown). In principle, calcium would ionically interact with two neighbouring carboxylic acids, inducing a cross-linkage of the conjugate. The mean size of the camptothecin-loaded nanoparticles when manufactured with G-HPCD appeared to be slightly higher than that obtained with G-mPEG (Table 3). In a similar way, nanoparticles from G-mPEG displayed a higher capability to load camptothecin than nanoparticles from G-HPCD (11 vs 8.6 μg/mg). Interestingly, for both types of nanoparticles (G-mPEG-NP and G-HPCD-NP) the drug loading was significantly higher than for unmodified Gantrez nanoparticles (about 2.2 μg/mg; data not shown). On the contrary, the CPT loading of G-HPCD-NP was about 6-times lower than that obtained by the direct encapsulation of cyclodextrin-drug complexes in Gantrez nanoparticles (Huarte et al., 2016).

Concerning the in vitro release of camptothecin from these nanoparticles, it is noteworthy that under simulated gastric conditions (SGC), just a small fraction of the loaded drug was released. Thus, 2-h of incubation in SGC induced a release of about 10% of the loaded drug with G-mPEG-NP and 20% for G-HPCD-NP. Under these pH conditions, the conjugates would be in their non-ionized form, favouring a compact formation of the nanoparticle and, minimizing the release of the drug. However, when nanoparticles were incubated in simulated intestinal fluid (neutral pH conditions), practically the total cargo (80% for G-mPEG-NP and 90% for G-HPCD-NP) was released in the first 60 min. This observation would be directed related with the swelling of nanoparticles promoted by the ionization of carboxylic acid groups of the copolymers as well as by the presence of phosphates, which are well known by their ability to sequestrate calcium ions (Kaliappan and Lucey, 2011), especially under neutral and basic pH conditions (Fredd and Fogler, 1998).

In the biodistribution studies, G-mPEG-NP and G-HPCD-NP displayed a different fate within the ileum mucosa than Gantrez nanoparticles. Thus, conventional nanoparticles appear to remain trapped in the mucus layer, whereas nanoparticles from conjugates were capable to

Table 4
Pharmacokinetic parameters estimated after a single dose (1 mg/kg) of an oral CPT suspension and the equivalent CPT dose of con-mPEG2-NP or con-HPCD-NP orally. Data expressed as mean (±SD), (n = 6).

	Dose (mg/kg)	AUC (μg h/mL)	C_{max} (μg/mL)	T_{max} (h)	$t_{1/2z}$ (h)	Cl (mL/h)	V (mL)	Fr
CPT suspension	1	0.38 ± 0.21	0.08 ± 0.02	0.5	1.6 ± 0.8	619 ± 357	1545 ± 414	1
G-mPEG-NP	1	2.9 ± 0.5*,†	0.08 ± 0.03	0.5	28 ± 9.6**	54 ± 9**,†	2181 ± 857	7.6
G-HPCD-NP	1	1.1 ± 0.4*	0.08 ± 0.05	0.5	12.7 ± 7.4*	180 ± 45*	1813 ± 518	2.9

AUC: area under the concentration-time curve from time 0 to t h; C_{max}: peak plasma concentration; T_{max}: time to peak plasma concentration; $t_{1/2z}$: half-life of the terminal phase; Cl: clearance; V: volumen of distribution; Fr: relative oral bioavailability. *$p < 0.05$, ** $p < 0.01$ oral CPT suspension vs. nanoparticle formulations (G-mPEG-NP and G-HPCD-NP). (†) $p < 0.05$ G-HPCD-NP vs. G-mPEG-NP.

reach the surface of the intestinal epithelium (Fig. 4). These observations would confirm that the surface of nanoparticles from conjugates is different to that of the original poly(anhydride). It is possible to hypothesize that the hydrophilic areas of conjugates would be oriented through the external aqueous phase forming a hydrophilic corona on the surface of nanoparticles and, thus, conferring the capability to diffuse through the mucus layer and reach the enterocytes. In the recent past, pegylation of nanoparticles have been described as an adequate strategy to minimise their interaction with the lumen contents (Suk et al., 2016), and to improve their capability to diffuse within the protective mucus layers (Inchaurraga et al., 2015; Bourganis et al., 2015). In a similar way, nanoparticles encapsulating cyclodextrins would show a higher ability to penetrate in the mucus layer than conventional poly(anhydride) nanoparticles (Calleja et al., 2014).

The oral administration of camptothecin after its encapsulation in the Gantrez-based nanoparticles displayed prolonged and sustained plasma levels of the anticancer drug for at least 48 h (Fig. 5). Therefore, these nanoparticles offered a higher AUC than the traditional aqueous drug suspension. In fact, G-HPCD-NP and G-mPEG-NP improved 2.9- and 7.6-times the oral relative bioavailability, compared with the drug suspension, respectively (Table 4). The improvement of the relative oral bioavailability provided for G-HPCD-NP was 2-times lower than that provided by nanoparticles prepared by the encapsulation of cyclodextrin-drug complexes (Huarte et al., 2016). In any case, the CPT oral bioavailability obtained for G-mPEG-NP was between 2- and 3-times higher than previous data reported in the literature employing solid lipid nanoparticles (Du et al., 2018), poly(amido amine) dendrimers (Sadekar et al., 2013) or deoxycholic acid-CPT conjugate (Xiao et al., 2019).

Another important aspect related with these nanoparticles would be their effect on the drug's primary parameters. Thus, when camptothecin was orally administered in the form of nanoparticles, its half-life in plasma ($t_{1/2z}$) and volume of distribution increased as compared with the suspension. In addition, the anticancer drug clearance was significantly lower when formulated in the form of nanoparticles (G-mPEG-NP and G-HPCD-NP) than when prepared as a traditional aqueous suspension (Table 4). These findings would be explained by the protective effect of these nanoparticles against both the drug's elimination in the gut and its conversion into the inactive carboxylate form. In the former, these nanoparticles (as observed in the biodistribution studies) would be capable to carry their cargo to the surface of the enterocyte, in which they would release their content, increasing the residence time of nanoparticles within the gut. In parallel, the presence of either PEG or HP-β-CD residues would disturb the activity of the intestinal P-gp, improving the absorbed fraction of the given dose. In the latter, the reported ability of PEGs and HP-β-CD to stabilize the lactone form of camptothecin would maintain the anticancer drug in its active form until its absorption. All together would result in nanoparticles capable to lengthen the camptothecin half-life and prolong the bioavailability of the active lactone form. This approach would be in line with an improved efficacy of this anticancer drug. In fact, it has been described that a prolonged and sustained Topo 1 inhibition (including with daily low-dose dosing regimens) can mediate a hypoxia-inducible factor 1 alpha (HIF-1) inhibition mechanism, augmenting the efficacy of the anticancer drug (Rapisarda et al., 2004; Leonard et al., 2017).

In summary, the modification of Gantrez™ AN with hydrophilic excipients such as mPEG and HPCD may be a suitable strategy to simplify the preparative process of nanoparticles, providing mucopenetrating properties and the ability to increase the oral bioavailability of certain drugs, particularly those that are substrates of intestinal P-gp. In the particular case of camptothecin, the G-mPEG-based nanoparticles demonstrated a superior ability to promote its oral absorption than the G-HPCD-based nanoparticles.

Credit author statement

Judit Huarte: Acquisition of data, analysis and/or interpretation of data, Writing- original draft preparation.

Socorro Espuelas: Conceptualization, methodology.

Cristina Martínez-Oharriz: Methodology, analysis and/or interpretation of data.

Juan M. Irache: Conceptualization, Writing- Reviewing.

Declaration of Competing Interest

The authors declare that they have no known competing financial interests or personal relationships that could have appeared to influence the work reported in this paper.

Acknowledgements

Judit Huarte was also financially supported by a grant from Asociación de Amigos de la Universidad de Navarra and from the 7th Framework Programme's Project 295218 of the International Research Staff Exchange Scheme (IRSES), Marie Curie Actions.

Appendix A. Supplementary data

Supplementary data to this article can be found online at https://doi.org/10.1016/j.ijpx.2021.100104.

References

Adane, E.D., Liu, Z., Xiang, T.X., Anderson, B.D., Leggas, M., 2012. Pharmacokinetic modeling to assess factors affecting the oral bioavailability of the lactone and carboxylate forms of the lipophilic camptothecin analogue AR-67 in rats. Pharmaceut. Res. 29 (7), 1722–1736. https://doi.org/10.1007/s11095-011-0617-0.

Arbós, P., Arangoa, M.A., Campanero, M.A., Irache, J.M., 2002. Quantification of the bioadhesive properties of protein-coated PVM/MA nanoparticles. Int. J. Pharmaceut. 242, 129–136. https://doi.org/10.1016/s0378-5173(02)00182-5.

Botella, P., Rivero-Buceta, E., 2017. Safe approaches for camptothecin delivery: Structural analogues and nanomedicines. J. Control. Release 247, 28–54. https://doi.org/10.1016/j.jconrel.2016.12.023.

Bourganis, V., Karamanidou, T., Samaridou, E., Karidi, K., Kammona, O., Kiparissides, C., 2015. On the synthesis of mucus permeating nanocarriers. Eur. J. Pharmaceut. Biopharmaceut. 97 (Pt A), 239–249. https://doi.org/10.1016/j.ejpb.2015.01.021.

Calleja, P., Espuelas, S., Corrales, L., Pio, R., Irache, J.M., 2014. Pharmacokinetics and antitumor efficacy of paclitaxel-cyclodextrin complexes loaded in mucus-penetrating nanoparticles for oral administration. Nanomedicine (London) 9 (14), 2109–2121. https://doi.org/10.2217/nnm.13.199.

Calvo, J., Lavandera, J.L., Agüeros, M., Irache, J.M., 2011. Cyclodextrin/poly(anhydride) nanoparticles as drug carriers for the oral delivery of atovaquone. Biomed. Microdevices 13 (6), 1015–1025. https://doi.org/10.1007/s10544-011-9571-1.

Champoux, J.J., 2001. DNA topoisomerases: structure, function, and mechanism. Annu. Rev. Biochem. 70, 369–413. https://doi.org/10.1146/annurev.biochem.70.1.369.

Ci, T., Li, T., Chang, G., Yu, L., Ding, J., 2013. Simply mixing with poly(ethylene glycol) enhances the fraction of the active chemical form of antitumor drugs of camptothecin family. J. Control. Release 169 (3), 329–335. https://doi.org/10.1016/j.jconrel.2012.12.004.

De Cesare, M., Pratesi, G., Veneroni, S., Bergottini, R., Zunino, F., 2004. Efficacy of the Novel Camptothecin Gimatecan against Orthotopic and Metastatic Human Tumor Xenograft Models. Clin. Cancer Res. 10 (21), 7357–7364. https://doi.org/10.1158/1078-0432.CCR-04-0962.

Dev, S., Dhaneshwar, S.R., Mathew, B., 2016. Discovery of camptothecin based topoisomerase I inhibitors: Identification using an atom based 3D-QSAR, pharmacophore modeling, virtual screening and molecular docking approach. Comb. Chem. High Throughput Screen. 19 (9), 752–763. https://doi.org/10.2174/1386207319666160810154346.

Du, Y., Ling, L., Ismail, M., He, W., Xia, Q., Zhou, W., Yao, C., Li, X., 2018. Redox sensitive lipid-camptothecin conjugate encapsulated solid lipid nanoparticles for oral delivery. Int. J. Pharmaceut. 549 (1–2), 352–362. https://doi.org/10.1016/j.ijpharm.2018.08.010.

Fox, M.E., Guillaudeu, S., Fréchet, J.M.J., Jerger, K., Macaraeg, N., Szoka, F.C., 2009. Synthesis and in vivo antitumor efficacy of PEGylated poly(L-lysine) dendrimer-camptothecin conjugates. Mol. Pharmaceut. 2, 3888–3890. https://doi.org/10.1021/mp9001206.

Fredd, C., Fogler, H., 1998. The influence of chelating agents on the kinetics of calcite dissolution. J. Colloid Interface Sci. 204, 187–197. https://doi.org/10.1006/jcis.1998.5535.

Huarte, J., Espuelas, S., Lai, Y., He, B., Tang, J., Irache, J.M., 2016. Oral delivery of camptothecin using cyclodextrin/poly(anhydride) nanoparticles. Int. J. Pharmaceut. 506 (1–2), 116–128. https://doi.org/10.1016/j.ijpharm.2016.04.045.

Inchaurraga, L., Martín-Arbella, N., Zabaleta, V., Quincoces, G., Peñuelas, I., Irache, J.M., 2015. In vivo study of the mucus-permeating properties of PEG-coated nanoparticles following oral administration. Eur. J. Pharmaceut. Biopharmaceut. 97 (Pt A), 280–289. https://doi.org/10.1016/j.ejpb.2014.12.021.

Inchaurraga, L., Martínez-López, A.L., Cattoz, B., Griffiths, P.C., Wilcox, M., Pearson, J. P., Quincoces, G., Peñuelas, I., Martin-Arbella, N., Irache, J.M., 2019. The effect of thiamine-coating nanoparticles on their biodistribution and fate following oral administration. Eur. J. Pharmaceut. Sci. 128, 81–90. https://doi.org/10.1016/j.ejps.2018.11.025.

Kaliappan, S., Lucey, J.A., 2011. Influence of mixtures of calcium-chelating salts on the physicochemical properties of casein micelles. J. Dairy Sci. 94, 4255–4263. https://doi.org/10.3168/jds.2010-3343.

Leonard, S.C., Lee, H., Gaddy, D.F., Klinz, S.G., Paz, N., Kalra, A.V., Drummond, D.C., Chan, D.C., Bunn, P.A., Fitzgerald, J.B., Hendriks, B.S., 2017. Extended topoisomerase 1 inhibition through liposomal irinotecan results in improved efficacy over topotecan and irinotecan in models of small-cell lung cancer. Anti-Cancer Drugs 28 (10), 1086–1096. https://doi.org/10.1097/CAD.0000000000000545.

Li, C., Wallace, S., 2008. Polymer-drug conjugates: recent development in clinical oncology. Adv. Drug Deliv. Rev. 60 (8), 886–898. https://doi.org/10.1016/j.addr.2007.11.009.

Li, Q.Y., Zu, Y.G., Shi, R.Z., Yao, L.P., 2006. Review camptothecin: current perspectives. Curr. Med. Chem. 13 (17), 2021–2039. https://doi.org/10.2174/092986706777585004.

Li, F., Jiang, T., Li, Q., Ling, X., 2017. Camptothecin (CPT) and its derivatives are known to target topoisomerase I (Top1) as their mechanism of action: did we miss something in CPT analogue molecular targets for treating human disease such as cancer? Am. J. Cancer Res. 7 (12), 2350–2394.

Liu, L.F., Desai, S.D., Li, T.K., Mao, Y., Sun, M., Sim, S.P., 2000. Mechanism of action of camptothecin. Ann. N. Y. Acad. Sci. 922, 1–10. https://doi.org/10.1111/j.1749-6632.2000.tb07020.x.

Lorence, A., Nessler, C.L., 2004. Camptothecin, over four decades of surprising findings. Phytochemistry 65, 2735–2749. https://doi.org/10.1016/j.phytochem.2004.09.001.

Lucio, D., Martínez-Ohárriz, M.C., Gu, Z., He, Y., Aranaz, P., Vizmanos, J.L., Irache, J.M., 2018. Cyclodextrin-grafted poly(anhydride) nanoparticles for oral glibenclamide administration. In vivo evaluation using *C. elegans*. Int. J. Pharmaceut. 547 (1–2), 97–105. https://doi.org/10.1016/j.ijpharm.2018.05.064.

Malhotra, S., Dumoga, S., Joshi, A., Mohanty, S., Singh, N., 2021. Polymeric micelles coated with hybrid nanovesicles enhance the therapeutic potential of the reversible topoisomerase inhibitor camptothecin in a mouse model. Acta Biomater. 121, 579–591. https://doi.org/10.1016/j.actbio.2020.11.049.

Mazo, P.C., Estenoz, D., Ríos, L.A., 2011. Kinetics of the esterification of maleic anhydride with castor oil. Lat. Am. Appl. Res. 41 (1), 11–15.

Negi, L.M., Tariq, M., Talegaonkar, S., 2013. Nano scale self-emulsifying oil based carrier system for improved oral bioavailability of camptothecin derivative by P-Glycoprotein modulation. Colloids Surf. B: Biointerfaces 111, 346–353. https://doi.org/10.1016/j.colsurfb.2013.06.001.

Nguyen, T.T.L., Duong, V.A., Maeng, H.J., 2021. Pharmaceutical formulations with P-glycoprotein inhibitory effect as promising approaches for enhancing oral drug absorption and bioavailability. Pharmaceutics. 13, 1103. https://doi.org/10.3390/pharmaceutics13071103.

Oberlies, N.H., Kroll, D.J., 2004. Camptothecin and taxol: historic achievements in natural products research. J. Nat. Prod. 67, 129–135. https://doi.org/10.1021/np030498t.

Pommier, Y., 2006. Topoisomerase I inhibitors: camptothecins and beyond. Nat. Rev. Cancer 6, 789–802. https://doi.org/10.1038/nrc1977.

Rapisarda, A., Zalek, J., Hollingshead, M., Braunschweig, T., Uranchimeg, B., Bonomi, C. A., Borgel, S.D., Carter, J.P., Hewitt, S.M., Shoemaker, R.H., Melillo, G., 2004. Schedule-dependent inhibition of hypoxia-inducible factor-1alpha protein accumulation, angiogenesis, and tumor growth by topotecan in U251-HRE glioblastoma xenografts. Cancer Res. 64, 6845–6848. https://doi.org/10.1158/0008-5472.CAN-04-2116.

Ruiz-Gatón, L., Espuelas, S., Larrañeta, E., Reviakine, I., Yate, L.A., Irache, J.M., 2018. Pegylated poly(anhydride) nanoparticles for oral delivery of docetaxel. Eur. J. Pharmaceut. Sci. 118, 165–175. https://doi.org/10.1016/j.ejps.2018.03.028.

Sadekar, S., Thiagarajan, G., Bartlett, K., Hubbard, D., Ray, A., McGill, L.D., Ghandehari, H., 2013. Poly(amido amine) dendrimers as absorption enhancers for oral delivery of camptothecin. Int. J. Pharmaceut. 456 (1), 175–185. https://doi.org/10.1016/j.ijpharm.2013.07.071.

Saetern, A.M., Nguyen, N.B., Bauer-Brandl, A., Brandl, M., 2004. Effect of hydroxypropyl-beta-cyclodextrin-complexation and pH on solubility of camptothecin. Int. J. Pharmaceut. 284, 61–68. https://doi.org/10.1016/j.ijpharm.2004.07.014.

Sanoff, H.K., Moon, D.H., Moore, D.T., Boles, J., Bui, C., Blackstock, W., O'Neil, B.H., Subramaniam, S., McRee, A.J., Carlson, C., Lee, M.S., Tepper, J.E., Wang, A.Z., 2019. Phase I/II trial of nano-camptothecin CRLX101 with capecitabine and radiotherapy as neoadjuvant treatment for locally advanced rectal cancer. Nanomedicine. 18, 189–195. https://doi.org/10.1016/j.nano.2019.02.021.

Suk, J.S., Xu, Q., Kim, N., Hanes, J., Ensign, L.M., 2016. PEGylation as a strategy for improving nanoparticle-based drug and gene delivery. Adv. Drug Deliv. Rev. 99 (Pt A), 28–51. https://doi.org/10.1016/j.addr.2015.09.012.

Swaminathan, S., Pastero, L., Serpe, L., Trotta, F., Vavia, P., Aquilano, D., Trotta, M., Zara, G., Cavalli, R., 2010. Cyclodextrin-based nanosponges encapsulating camptothecin: physicochemical characterization, stability and cytotoxicity. Eur. J. Pharmaceut. Biopharmaceut. 74 (2), 193–201. https://doi.org/10.1016/j.ejpb.2009.11.003.

Takemoto, I., Itagaki, S., Chiba, M., Itoh, T., Hirano, T., Iseki, K., 2006. Characterization of secretory intestinal transport of the lactone form of CPT-11. Cancer Chemother. Pharmacol. 57 (1), 129–133. https://doi.org/10.1007/s00280-005-0042-3.

Ünal, S., Aktaş, Y., Benito, J.M., Bilensoy, E., 2020. Cyclodextrin nanoparticle bound oral camptothecin for colorectal cancer: Formulation development and optimization. Int. J. Pharmaceut. 584, 119468. https://doi.org/10.1016/j.ijpharm.2020.119468.

Van Hattum, A.H., Pinedo, H.M., Schlueper, H.M.M., Erkelens, C.A.M., Tohgo, A., Boven, E., 2002. The activity profile of the hexacyclic camptothecin derivative DX-8951f in experimental human colon cancer and ovarian cancer. Biochem. Pharmacol. 64, 1267–1277. https://doi.org/10.1016/s0006-2952(02)01297-2.

Venditto, V.J., Simanek, E.E., 2010. Cancer therapies utilizing the camptothecins: a review of the in vivo literature. Mol. Pharmaceut. 7 (2), 307–349. https://doi.org/10.1021/mp900243b.

Werle, M., 2008. Natural and synthetic polymers as inhibitors of drug efflux pumps. Pharmaceut. Res. 25 (3), 500–511. https://doi.org/10.1007/s11095-007-9347-8.

Xiao, L., Zhou, Y., Zhang, X., Ding, Y., Li, Q., 2019. Transporter-targeted bile acid-camptothecin conjugate for improved oral absorption. Chem. Pharmaceut. Bull. (Tokyo). 67 (10), 1082–1087. https://doi.org/10.1248/cpb.c19-00341.

Yang, S., Zhu, J., Lu, Y., Liang, B., Yang, C., 1999. Body distribution of camptothecin solid lipid nanoparticles after oral administration. Pharmaceut. Res. 16 (5), 751–757. https://doi.org/10.1023/a:1018888927852.

Zhang, J., Ma, P.X., 2013. Cyclodextrin-based supramolecular systems for drug delivery: recent progress and future perspective. Adv. Drug Deliv. Rev. 65 (9), 1215–1233. https://doi.org/10.1016/j.addr.2013.05.001.

Zhang, Y., Meng, F.C., Cui, Y.L., Song, Y.F., 2011. Enhancing effect of hydroxypropyl-beta-cyclodextrin on the intestinal absorption process of genipin. J. Agric. Food Chem. 59, 10919–10926. https://doi.org/10.1021/jf202712y.